

Propagation and Ghosts in the Classical Kagome Antiferromagnet

J. Robert,¹ B. Canals,² V. Simonet,² and R. Ballou²

¹Laboratoire Léon Brillouin, CEA-CNRS, CE-Saclay, 91191 Gif-sur-Yvette, France

²Institut NEEL, CNRS & Université Joseph Fourier, BP 166, 38042 Grenoble Cedex 9, France
(Dated: November 29, 2018)

We investigate the classical spin dynamics of the kagome antiferromagnet by combining Monte Carlo and spin dynamics simulations. We show that this model has two distinct low temperature dynamical regimes, both sustaining propagative modes. The expected gauge invariance type of the low energy low temperature out of plane excitations is also evidenced in the non linear regime. A detailed analysis of the excitations allows to identify ghosts in the dynamical structure factor, i.e propagating excitations with a strongly reduced spectral weight. We argue that these dynamical extinction rules are of geometrical origin.

PACS numbers: 75.10Hk,75.40Gb,75.40Mg,75.50.Ee

Geometrical frustrated magnets are currently a source of high interest for the exotic phases and unexpected dynamics that they are liable to generate. A full insight about their behaviors is still far from having been acquired, in particular at the lowest temperatures.

A prototype is the classical Heisenberg kagome antiferromagnet [1]. As a basic distinctive feature of the geometrical frustration, its ground state consists in a continuous connected manifold of spin configurations. At high temperatures ($T/J \gtrsim 0.1$, with J the first neighbor exchange), the system is paramagnetic. It enters what we shall call from now on a cooperative magnetic phase in the range $5 \cdot 10^{-3} \lesssim T/J \lesssim 0.1$ where short range correlations are enhanced. At the lowest temperatures ($T/J \lesssim 5 \cdot 10^{-3}$), thermal fluctuations above each of the spin configurations of the ground state manifold are not equivalent and drive an entropic based order out of disorder mechanism [2], eventually selecting a spin plane [3] and developing an octupolar order [4]. We shall call this phase coplanar to distinguish it from the former. While in both low temperature regimes it was shown that spin pair correlations remain short ranged [5], it is only in the coplanar phase that the continuous degeneracy of the manifold was argued to be reduced to a discrete one, described by the 3-colorings of the lattice [6]. Altogether, these results provide a rather clear picture of the thermodynamics of the classical kagome antiferromagnet, which should apply to experimental compounds with large magnetic moments but also be of some relevance for low spin systems, since quantum fluctuations often play a significant role at very low temperatures only.

A much poorer understanding of the spin dynamics is in contrast available. To our knowledge, only one numerical investigation was so far conducted [7], which furthermore was not resolved in momentum vectors \mathbf{Q} , thus ignoring any diffusive or propagating aspects of the excitations. In this letter, we analyze the temperature dependent dynamics of the classical kagome antiferromagnet from two point of views. We first show that at low temperatures, spin waves (SW) do propagate and are sen-

sitive to the underlying spin texture, either cooperative paramagnetic or coplanar. Quantitative analysis of the dynamical structure factor is performed and provides the characteristic time scales. Additionally, the invariance of the linear SW spectra with respect to the ground state spin configurations on which they are built is evidenced in a wide range of temperatures, including those where non linear effects are at play. We next put forward that peculiar excitations develop that would be almost invisible to dynamical spin-pair correlations sensitive probes, such as inelastic neutron scattering.

The numerical method used in this work is a combination of an hybrid Monte Carlo (MC) method, which allows generating samples of spin arrays at a given temperature, and an integration of the non-linear coupled equations of motion for the spin dynamics (SD):

$$\frac{d\mathbf{S}_i}{dt} = J \left(\sum_j \mathbf{S}_j \right) \times \mathbf{S}_i, \quad (1)$$

where j is a first neighbor of i and $J > 0$ is the antiferromagnetic exchange [8]. The numerical integration has been performed up to $t = 1000 J^{-1}$ using an 8th-order Runge-Kutta method (RK) with an adaptative step-size control. The RK error parameter as well as the RK order have been fixed in order to preserve the euclidian distance with a test-full diffusion of Eq. 1 performed with the more robust but time consuming Burlisch-Stoer algorithm. As a result, trivial constants of motion, such as the total energy E_{tot} and magnetization M_{tot} , are conserved with a relative error smaller than 10^{-6} . As for the spin arrays samplings by the MC method, a first run has been performed in order to find an optimal set of temperatures for a parallel tempering scheme [9], which minimizes the ergodic time [10]. A reduction of the solid angle for each spin flip trial together with rotations around the local molecular fields ensure a rate acceptance above 40%. The numerical simulations reported in this work were performed on samples of $L \times L \times 3$ spins with $L = 36$ and periodic boundary conditions. Our interest lies in the

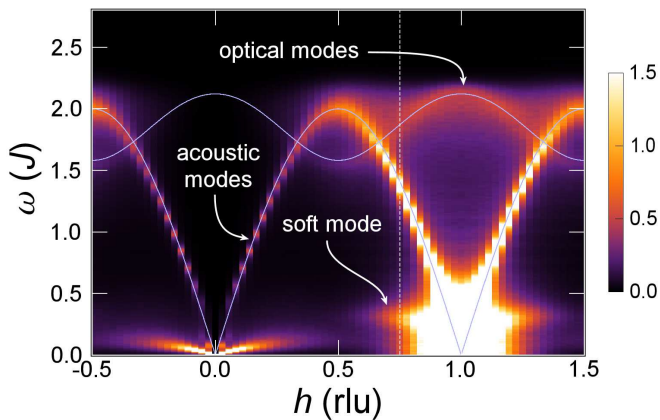


FIG. 1: (color online) Intensity map (*a.u.*) of the scattering function *vs.* ω and $\mathbf{Q} = (h, 0)$, for $T/J = 5 \cdot 10^{-4}$. The LSW dispersion relations $\omega(\mathbf{Q})$ for the phase $q = \sqrt{3} \times \sqrt{3}$ are plotted as blue lines. The white dotted line corresponds to the constant- \mathbf{Q} scans presented on Fig. 2.

scattering function, namely the time and space Fourier transform of the dynamical spin-pair correlations:

$$S(\mathbf{Q}, \omega) = \sum_{ij} \int \frac{dt}{\sqrt{2\pi N}} \langle \mathbf{S}_i(0) \cdot \mathbf{S}_j(t) \rangle e^{-i\mathbf{Q} \cdot \mathbf{R}_{ij}} e^{-i\omega t} \quad (2)$$

where \mathbf{Q} and ω are the momentum vector and energy transfer, $\langle \dots \rangle$ is the ensemble average, $\mathbf{R}_{ij} = \mathbf{R}_j - \mathbf{R}_i$ and N the number of spins.

Details about static properties will not be given here. It however is worth noting that our results for $\omega = 0$ at very low temperatures ($T/J \lesssim 5 \cdot 10^{-3}$), when entropic selection is at work, points towards fluctuations predominantly associated with the so-called $q = \sqrt{3} \times \sqrt{3}$ phase. This meets with previous conclusions, although those were inferred from instantaneous ensemble averages [5, 6, 11]. We similarly got very good agreements with previous numerical or analytical investigations of the specific heat, the coplanar ordering, or the instantaneous scattering function [3, 4, 5, 12], giving confidence on the quality of our numerical simulations.

Let us now focus on the dynamical properties of the kagome antiferromagnet. Although the propagation of collective excitations may appear unexpected in such a system, where the spin-pair correlation function decays exponentially with distance at finite temperatures [5], a sufficient temporal and spatial stiffness may lead to the propagation of SW in locally ordered regions. Therefore, a required condition for the development of SW excitations is an increase with decreasing temperature of the autocorrelation time τ_a featuring the lifetime of locally ordered states. τ_a has been numerically evaluated by integrating the scattering function over all \mathbf{Q} -values in the reciprocal space, which gives access to the time Fourier transform of the autocorrelation function $A(t) = \langle \mathbf{S}_i(0) \cdot \mathbf{S}_i(t) \rangle$. A fit of the obtained quasielas-

tic (QE) signal using a lorentzian shape $\frac{I_0 \Gamma_a}{\Gamma_a^2 + \omega^2}$, associated with a decaying exponential law $A(t) = \exp(-\Gamma_a t)$ in time space, allows extracting the Half Width at Half Maximum (HWHM) $\Gamma_a \propto 1/\tau_a$. As the temperature is decreased, this shows an algebraic variation $\Gamma_a = \mathcal{A}T^\zeta$ with $\zeta = 0.995 \pm 0.018$ for $T/J \lesssim 0.1$ (see Fig. 3a), transposing to a slowing down of the spin fluctuations, but nevertheless no spin freezing even at temperatures as low as $T/J = 5 \cdot 10^{-4}$. Interestingly, the same thermal variation is observed in the cooperative paramagnetic ($T/J \gtrsim 5 \cdot 10^{-3}$) and the coplanar states ($T/J \lesssim 5 \cdot 10^{-3}$) regimes, asserting that the entropic selection favoring the coplanar manifold has no influence on the lifetime τ_a of locally ordered states. Now that we have characterized the temporal stiffness associated with the T^{-1} slowing down of τ_a , we address the question of well defined excitations as well as their possible propagation. An evidence of the existence of SW-type excitations at low temperatures is explicit in the excitation spectrum for $T/J = 5 \cdot 10^{-4}$ (see Fig. 1). For comparison, the linear spin wave (LSW) spectrum [11] emerging from the pure $q = \sqrt{3} \times \sqrt{3}$ phase is shown. The SD simulations evidence a large weight of $S(\mathbf{Q}, \omega)$ at this LSW spectrum, confirming that the $q = \sqrt{3} \times \sqrt{3}$ short range dynamical correlations are favored at very low temperature.

The analysis of the spectrum as a function of the temperature allows getting more insights about the formation of the SW excitations. We show in Fig. 2 the frequency dependence of $S(\mathbf{Q}, \omega)$ at the point $\mathbf{Q}_0 = 2\pi(3/4, 0)$ in the reciprocal space, located between the Brillouin zone (BZ) boundary and the BZ center (see Fig. 1), where the soft, acoustic and optical modes are particularly easy to distinguish. These constant- \mathbf{Q} scans are

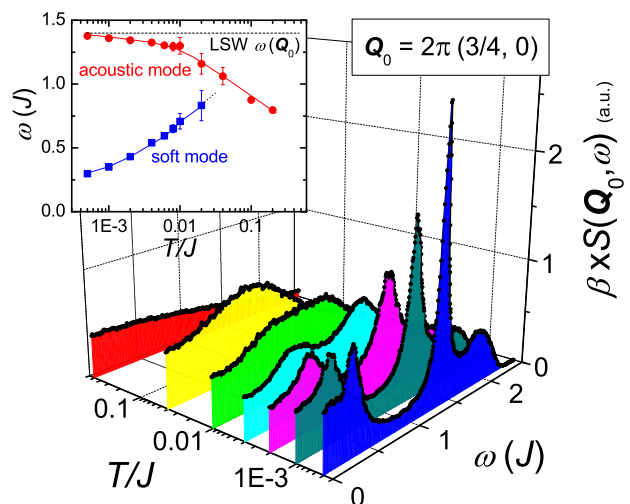


FIG. 2: (color online) Temperature weighted scattering function *vs.* energy at different temperatures for $\mathbf{Q}_0 = 2\pi(3/4, 0)$. Inset : position of soft and acoustic modes versus temperature; error bars obtained from several fitting processes.

represented for temperatures from $T/J = 0.5$ to $5 \cdot 10^{-4}$. At high temperatures ($T/J \gtrsim 0.2$), only a QE signal centered at $\omega = 0$ contributes to the scattering function $S(\mathbf{Q}, \omega)$. A single broad excitation at finite energy comes into sight on decreasing T/J from 0.2 to 10^{-2} , although strongly softened compared to the LSW theory expectation (see inset of Fig. 2). Below $T/J = 10^{-2}$, the broad peak splits into two excitations, respectively associated with the SW acoustic modes and the emerging soft modes, gradually separating from each other and getting thinner as the temperature goes down (see Fig. 2). The softening of the modes dies away to disappear below $T/J = 5 \cdot 10^{-4}$. The soft mode, expected to be non-dispersive in LSW theory, is here observed at finite energy, due to the non linear nature of Eq. 1, which takes account of the interactions between the SW. This effect is expected to decrease with temperature, which is consistent with the fact that the soft mode drops to zero energy when temperature goes down (inset of Fig. 2). Finally, one can discern an additional peak at $\omega \simeq 2J$ for $T/J < 2 \cdot 10^{-3}$, corresponding to optical modes.

Each mode i of the excitation spectrum can be characterized by its dispersion relation $\omega^i(\mathbf{Q})$, its lifetime $\tau_{SW}^i \propto (\Gamma_{SW}^i)^{-1}$, and its intensity I_0^i , all these quantities being accessible by fitting the excitation spectrum at different temperatures and \mathbf{Q}_0 values. Assuming Lorentzian shape for magnetic excitations, the scattering function writes :

$$S(\mathbf{Q}_0, \omega) = \sum_i \frac{I_0^i \Gamma^i}{(\Gamma^i)^2 + (\omega \pm \omega^i(\mathbf{Q}_0))^2} \quad (3)$$

where i runs over soft, acoustic and optical magnetic peaks for a particular \mathbf{Q}_0 value. We show Fig. 3b the thermal variation of the resulting SW HWHM $\Gamma_{SW} \propto \tau_{SW}^{-1}$ for $\mathbf{Q}_0 = 2\pi(3/4, 0)$. It is found out, contrarily to τ_a (see Fig. 3a), that τ_{SW} follows two distinct regimes below and above $T/J = 5 \cdot 10^{-3}$, both consistent with an algebraic law $\tau_{SW} = \mathcal{A}T^{-\zeta}$. τ_{SW} is in principle reduced by two physical processes. The first, common to all magnetic systems, is associated to the thermal fluctuations and anharmonic interactions between SW modes. In a disordered medium, this process is overwhelmed by a second one, induced by the motion of the system between the different ground states. In other words, even in the linear approximation, one is left with a set of linear equations of motions with time dependent initial conditions, the time variations of those being set by the autocorrelation time τ_a . In the pyrochlore antiferromagnet, it has been shown that τ_a is also proportional to T^{-1} and based on the above interpretation, it was proposed that the SW lifetime τ_{SW} is proportional to $T^{-1/2}$ [13]. This behavior is expected at least in the cooperative paramagnetic regime. In the corresponding temperature range, we find $\zeta = 0.18 \pm 0.07$, which is much lower than 1/2. In the low T regime, due to the selection of coplanar spin configurations, the out-of-plane

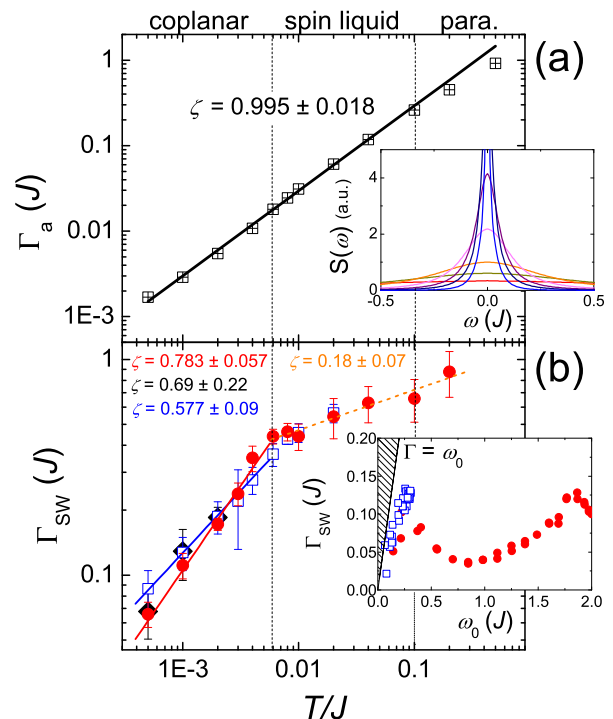


FIG. 3: (color online) (a) $\Gamma_a \propto \tau_a^{-1}$ obtained by fitting the QE signal $S(\omega)$, shown in the inset at several temperatures from $T/J = 0.5$ to $5 \cdot 10^{-4}$. (b) $\Gamma_{SW} \propto \tau_{SW}^{-1}$ for the soft (blue squares), in-plane (black diamonds) and out-of-plane (red circles) acoustic modes for $\mathbf{Q}_0 = 2\pi(3/4, 0)$. The error bars have been obtained by averaging over different fitting processes. If not seen, they are smaller than the symbols. The inset displays Γ_{SW} as a function $\omega_0 = \omega(\mathbf{Q})$, *ie* for several \mathbf{Q} -values. The hatched region forbids propagating excitations.

$\omega^\perp(\mathbf{Q})$ and the in-plane $\omega^\parallel(\mathbf{Q})$ modes become different, which allows distinguishing the corresponding scattering process $S(\mathbf{Q}, \omega) = S^\perp(\mathbf{Q}, \omega) + S^\parallel(\mathbf{Q}, \omega)$. Within the LSW, or equivalently at very low temperatures, the out of plane scattering function $S^\perp(\mathbf{Q}, \omega)$ is gauge invariant like, *ie* does not depend on the three coloring state on top of which the excitations develop (see Fig. 4b, left). Conversely, the in-plane contribution $S^\parallel(\mathbf{Q}, \omega)$ differs for each configuration it is built on (see Fig. 4b, right). In this coplanar regime, τ_{SW} seems to behave in similar ways for the in-plane ($\zeta = 0.69 \pm 0.22$) and out-of-plane ($\zeta = 0.783 \pm 0.057$) acoustic modes, whereas ζ is slightly weaker for the soft mode ($\zeta = 0.577 \pm 0.09$). Thereby, we clearly see two distinct dynamical regimes with a ζ value in the coplanar phase significantly larger than the value in the cooperative paramagnetic phase. This suggests that the SW lifetime is sensitive to the entropic selection of the coplanar manifold, that latter inducing some kind of stiffness in the spin texture. We can also wonder about the propagation of these magnetic excitations. If $\Gamma_{SW}/\omega_0 < 1$ for a given mode, it can be considered as a propagative SW, its lifetime τ_{SW} being longer than its

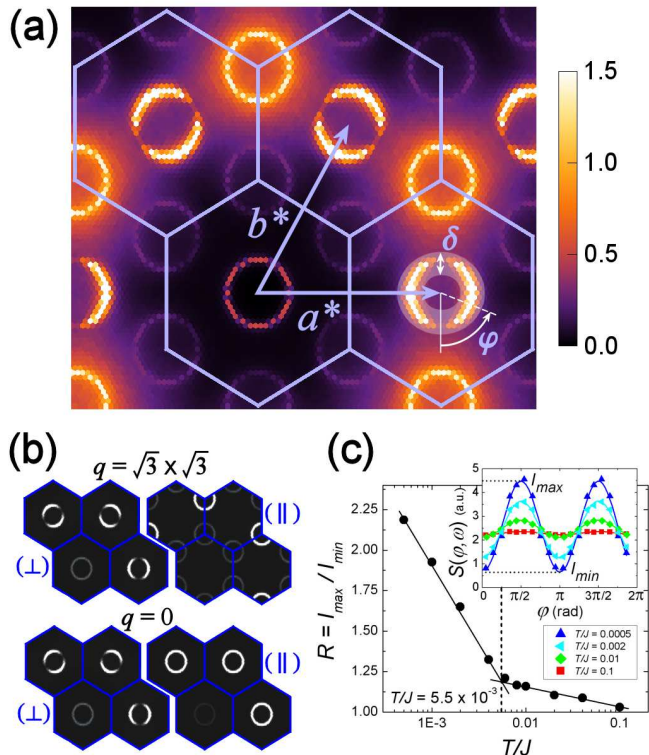


FIG. 4: (color online) (a) Intensity map (a.u.) in reciprocal space for $\omega = J$ and $T/J = 5 \cdot 10^{-4}$. The first and neighboring BZ are in blue. (b) Out-of-plane (\perp) (left) and in-plane (\parallel) (right) components for $q = \sqrt{3} \times \sqrt{3}$ and $q = 0$ spin configurations. (c) Anisotropy parameter $R = I_{max}/I_{min}$ vs. temperature. Inset : scattering function plotted for different temperatures in function of φ , as defined in Fig. (a).

period ω_0^{-1} . This actually is the case for the soft and acoustic modes, at least up to $T/J \lesssim 0.1$ (see inset of Fig. 3b for $T/J = 5 \cdot 10^{-4}$). This underlines that SW propagation in the kagome antiferromagnet, although of different nature, is possible in both regimes of cooperative paramagnetism and entropy induced coplanarity.

We finally focus on the spectral weight distribution in reciprocal space, which is non-uniform for the excitations emerging from the BZ centers, *i.e.* the out-of-plane acoustic like modes. A two dimensional intensity map in reciprocal space is shown in Fig. 4a, for $\omega = J$ and $T/J = 5 \cdot 10^{-4}$. The spectral weight $S(\mathbf{Q}, J)$ reaches its maximum value I_{max} along \mathbf{a}^* , \mathbf{b}^* or $\mathbf{a}^* - \mathbf{b}^*$ axis, and fades out in each corresponding perpendicular direction (with an intensity I_{min}). This results in the presence of “ghosts” in the excitation rings, *i.e.* existing excitations with a strongly reduced cross section, that would be invisible *e.g.* in neutron scattering experiments. Parameterizing these rings by the angle φ and integrating over a small width δ of the ring (see Fig. 4a) allows to quantitatively analyze the spectral weight anisotropy as a function of the temperature. Fig. 4c displays the evo-

lution of the anisotropy parameter $R = I_{max}/I_{min}$ with the temperature. Strong discrepancies between the cooperative paramagnetic regime ($R \simeq 1$) and the entropy driven coplanar regime, in which the anisotropy strongly increases with decreasing temperature, are evidenced. At the lowest temperatures, where SW propagates onto a disordered manifold, the strongly fluctuating spin texture could therefore be expected to drive these extinctions. Actually, two distinct arguments rather support a purely geometrical origin. Firstly, out of plane excitations are gauge invariant like. Therefore, the fluctuating nature of the manifold should not play any role. Secondly, we have numerically computed $S(\mathbf{Q}, \omega)$ for configurations prepared in slightly distorted ordered $q = 0$ and $q = \sqrt{3} \times \sqrt{3}$ phases and performed a LSW expansion around these two phases (Fig. 4b). All calculations reproduce this spectral anisotropy, pointing out that the ghost excitations rather originate from the peculiar geometry of the lattice revealed by spin coplanarity.

In conclusion, the propagation of spatially structured collective excitations has been numerically evidenced and quantitatively studied in the classical kagome antiferromagnet. Although the SW exist in both cooperative paramagnetic and coplanar regimes, their lifetime was found very sensitive to the entropic selection occurring below $T/J = 5 \cdot 10^{-3}$, in contrast with the same inverse temperature dependence of the autocorrelation time in both regimes. At very low temperatures, these propagative modes possess a noteworthy non uniform spectral weight expressing effective dynamical extinction rules.

We would like to thank C. Henley and E. Bonet for helpful discussions. B.C. also thanks Shan-Ho Tsai for a useful correspondence at the early stages of this work.

-
- [1] C. Zeng, and V. Elser, Phys. Rev B **42**, 8436 (1990); C. Zeng, and V. Elser, Phys. Rev B **51**, 8318 (1995).
 - [2] J. Villain, Z. Phys. B **33**, 31 (1979).
 - [3] J. T. Chalker, P. C. W. Holdsworth, and E. F. Shender, Phys. Rev. Lett. **68**, 855 (1992).
 - [4] M. Zhitomirsky, <http://fr.arxiv.org/abs/0805.0676v1>.
 - [5] J. N. Reimers and A. J. Berlinsky, Phys. Rev. B **48**, 9539 (1993).
 - [6] D. A. Huse and A. D. Rutenberg, Phys. Rev. B **45**, 7536 (1992).
 - [7] A. Keren, Phys. Rev. Lett. **72**, 3254 (1994)
 - [8] S.-H. Tsai, A. Bunker, and D. P. Landau, Phys. Rev. B **61**, 333 (2000).
 - [9] K. Hukushima and K. Nemoto, J. Phys. Soc. Jpn. **65**, 1604 (1996).
 - [10] H. G. Katzgraber, S. Trebst, D. A. Huse and M. Troyer, J. Stat. Mech., P03018 (2006).
 - [11] A. B. Harris, C. Kallin, and A. J. Berlinsky, Phys. Rev. B **45**, 2899 (1992).
 - [12] D. A. Garanin and B. Canals, Phys. Rev. B **59**, 443 (1999).
 - [13] R. Moessner and J. T. Chalker, Phys. Rev. Lett. **80**, 2929

(1998); Phys. Rev. B **58**, 12049 (1998).